ISSN 8755-6839

SCIENCE OF **TSUNAMI HAZARDS**

Journal of Tsunami Society International

Volume 31 **Number 2** **2012**

THE INDIAN OCEAN TSUNAMI OF 26 DECEMBER 2004
Analysis of Seismic Source Mechanism

R Mazova[1], B Kisel'man[2], N Baranova[3] and L Lobkovsky[4]

ABSTRACT

Based on the keyboard model of tsunamigenic earthquakes, an analysis was performed of the physical aspects of the 26 December 2004 earthquake off Sumatra and of the seismic source of the great tsunami generated in the Indian Ocean. A simplified keyboard model with vertical displacements of keyboard blocks was used for the numerical simulation in defining the tsunami's generation source and, based on known bathymetry, its subsequent propagation across the Indian Ocean basin. The numerical simulation of the seismic source took into account the oblique character of subduction zone, which was characteristic for this particular earthquake. Furthermore, the analysis evaluated the different scenarios of keyboard blocks motions - corresponding to real seismic and hydro acoustic studies of the earthquake process - as reported in the literature. Adequateness of the calculations performed was verified by comparison of real altimetry records of satellite "Yason-1" with virtual altimetric record, obtained by us for each calculation. The computational analysis helped explain the complex character of the tsunami and of its propagation and energy flux distribution in the Indian Ocean basin.

Key Words: *Indian Ocean tsunami, numerical modeling, satellite altimetry, keyboard model*

[1] Professor, Dept. of Applied Mathematics, N.N. State Technical University, Nizhny Novgorod, Russia 603695
[2] Associate Professor, Dept. of Circuits & Telecommun, N.N. State Tech.Univ., Nizhny Novgorod, Russia, 603695
[3] Magister, Dept. of Applied Mathematics, N.N. State Technical University, Nizhny Novgorod, Russia 603695
[4] Professor, Lab. of Seismology, Institute of Oceanology, Russian Academy of Sciences, Moscow, Russia 117247

1. INTRODUCTION

Special interest was developed in distinguishing the source characteristics of the 26 December 2004 earthquake near Sumatra and of the catastrophic tsunami it generated in the Indian Ocean from other more conventional, tsunamigenic quakes in this region and elsewhere. Two main factors were of particular interest for this event, namely the unusual length of the source region - which extended for nearly 1400 km – and the duration of rupture, which lasted almost 10 minutes. Essentially, such extensive spatial-temporal features of the seismic source complicate the process of using seismographic data in estimating the possible far-field tsunami amplitudes through the use of conventional tsunami numerical simulation methods. The difficulty arises from the fact that seismographs also register reflected signals, which lead to delays in determining the preliminary source parameters with conventional method (Ishii et al. 2005). In contrast to the Pacific Ocean where there are several deep-water pressure sensors, which permit to collect deep-water tsunami amplitude, in the Indian Ocean there was only data from near-coastal tide gauges providing direct measurements of tsunami amplitude and such data often becomes available with considerable delays. Therefore, as one of more effective ways to trace in real time tsunami parameters in the open sea, appears to be through the use of satellite altimetry (Hirata et al. 2006).

The use of altimetric data obtained from satellites "Jason-1" and "Topex-Poseidon" (USA-France) in analysis and numerical simulation of generation and propagation of tsunami (Hirata et al. 2006; Titov et al., 2005) has confirmed that - as expected - parameters of the Indian Ocean 2004 tsunami are determined firstly by details of processes in the seismic source. As known, the process of tsunami formation depends on the character and dynamics of movements in the seismic-source zone, or more definitely, on the initial ocean floor displacements. Knowing the initial stress distribution determines essentially the character of the near-source crustal displacements of the tsunamigenic earthquake source. An earthquake occurs when stress on any part of contact surface overcomes the breaking point and the motion on it is accelerated. This process - depending on earthquake preparation time and initial stress level before seismic movement - will proceed in quite different ways. Tsunami waves generated by such process of vertical displacement will be quite different in each case. This is a fact that must be taken into account in analyzing tsunami mechanisms.

Subduction along the Sunda trench is oblique along the west coast of Sumatra as well as along the Nicobar and Andaman Islands. The slopes of the subduction zone are highly indented, with large segments formed by transcurrent faults passing up to the roof of the subducted plate. Such block structure changes in the subduction zone and permits the use of a keyboard model to deduce the initial seismic source for the purpose of simulating the generation and subsequent propagation of the tsunami (Lobkovsky et al. 2004). The sources of such earthquakes are usually connected with deformation and "shooting" at stress, releasing keyboard blocks with characteristic size near 100 km. Such model with alternative motions of keyboard blocks was successfully applied by this study to simulate the 26 December 2004 Indian Ocean tsunami (Lobkovsky et al. 2006a; Lobkovsky and Mazova, 2007). In particular, a numerical simulation was performed of the 'domino' effect when one of the 'shooting' keyboard blocks near the earthquake epicenter, excites the next keyboard blocks in what corresponds to a uniform character of the rupture motion along the source but with decrease of movement with distance. However, sometimes in the long source several keyboard blocks can be

"shooted" almost simultaneously and this powerful "chord" produces the formation of a huge earthquake source and as a consequence the appearance of giant tsunami (Lobkovsky 1988). Similar multi-block models of the seismic source have been then used by other researchers (Hirata et al. 2006; Ishii et al. 2005; Lay et al. 2005; Song et al. 2005; Wilson 2005).

More detailed numerical simulation was performed by the present study by using a keyboard (multi-block) seismic source located in zone of earthquake 26 December 2004 and generation and the subsequent propagation of the tsunami waves and energy flux distribution in the Indian Ocean basin. To support the analysis, several scenarios of alternative motions of keyboard blocks were used for the extended seismic source and comparisons of tsunami wave heights were performed for given points of the basin, with the results being verified by data obtained by satellite altimetry, by coastal tide gauges and by visual tsunami run-up measurements. Additional verification was also performed by detailed comparison with the results of other studies using the geometry of their model seismic sources.

2. NUMERICAL SIMULATION OF GENERATION OF TSUNAMI WAVES BY SEISMIC SOURCE COMPRISING VARIOUS NUMBERS OF KEYBOARD BLOCKS AND THEIR PROPAGATION

To describe the wave generation and propagation processes a nonlinear system of shallow water equations was used (Lobkovsky et al. 2006b) which for the given case can be presented as

$$\begin{cases} \vec{U}_t + \vec{U} \cdot grad\, \vec{U} + g \cdot grad\, \eta = \vec{F} \\ \eta_t + div\left((H + \eta - B)\vec{U}\right) = B_t \end{cases}$$

where η is the water surface displacement, H is the basin depth, u and v are the components of horizontal wave velocity,

$$\vec{F} = \begin{pmatrix} fv - g\dfrac{u\sqrt{u^2+v^2}}{Ch^2(H+\eta-B)} \\ -fu - g\dfrac{v\sqrt{u^2+v^2}}{Ch^2(H+\eta-B)} \end{pmatrix}, \qquad \vec{U} = \begin{pmatrix} u \\ v \end{pmatrix},$$

where $f = 2\Omega\cos\theta$ is the Coriolis parameter, Ω is the Earth angular velocity, θ is the Earth geographic latitude, g is the gravity acceleration, $Ch = \dfrac{(H+\eta-B)^{0.4}}{sh}$ is the Shezi coefficient, sh is the roughness coefficient, $B(x,y,t)$ describes the basin bottom motion.

To perform the numerical simulation a bathymetric map with one-minute isobath cross-section was used. The calculation region used for the numerical simulations was taken in the geographical square bounded by 10^0 S – 25^0 N, 70^0 – 110^0 E, with grid system that included 1501x 2701 points. By known step on coordinates it was found step on time for the whole basin.

2.1 Main Points of Numerical Simulation

The analysis of numerical simulation scenarios was performed based on results of the following studies (Ammon et al. 2005; Fine et al. 2005; Hirata et al. 2006; Ishii et al. 2005; Lay et al. 2005; Lobkovsky 1988; Nagarajan et al. 2006; Park et al. 2005; Titov et al. 2005). The present analysis used data from tide gauges and from altimetry of the USA-France satellite "Jason-1". As known, almost two hours after the initial earthquake shock, the low-orbit altimetric satellite "Jason-1" scanned the ocean surface for a distance of 1500 km from Sri-Lanka towards the Bay of Bengal. During a time period of 10 minutes, the satellite passed over the tsunami wave front and measured, with accuracy of several centimeters, the ocean surface profile along a 5 km width band along its track (Wilson 2005). The flight trajectory of satellite "Jason-1" is indicated by the white line in Fig. 1a.

In order to adequately evaluate the results of the numerical simulation for each of the chosen scenarios, comparisons were made between the actual data obtained by observations and the virtual altimetric record computed by us for each scenario. Additionally used in the evaluation were the records of functioning tide gauges in the region (Fig.1a) (Nagarajan et al. 2006). Fig. 1b shows the model's seismic source, comprising 13 keyboard blocks.

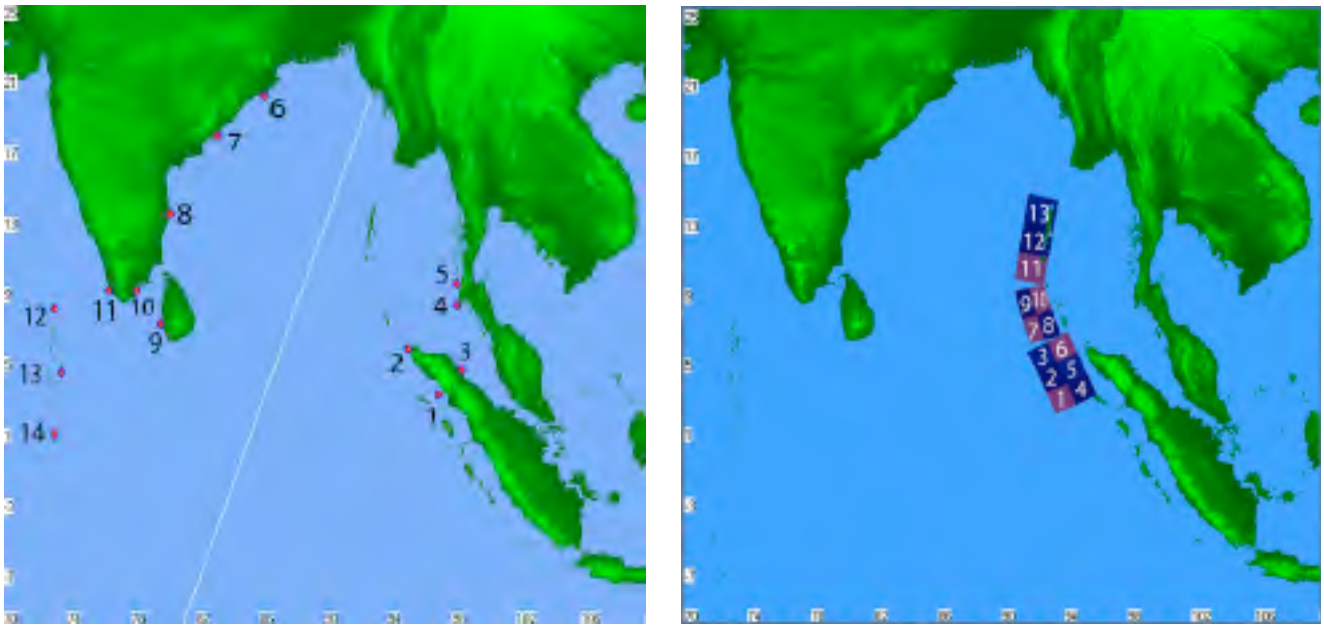

a) **b)**

Figures 1a and 1b. Maps of the region impacted by the Indian Ocean tsunami of 26 December 2004. Fig. 1a shows the locations of 14 model recording tide stations and the track of satellite "Jason-1" (white direct line). Fig. 1b shows the 13 keyboard blocks of the seismic source displacements that generated the tsunami. Of these, blocks 1-6 represent the Sumatra segment, 7-10 the Nicobar segment, and blocks 11-13 the Andaman segment.

2.2 Effect of seismic source length to characteristics of propagating tsunami wave and magnitude of wave heights along the coast

For the event of 26 December 2004 there exists an uncertainty in literature with source structure and seismic movements at all length of source. Therefore, it is of interest to study in details the dependence of characteristics of seismic source which generated long surface water wave. (cf. with (Lobkovsky 1988)).

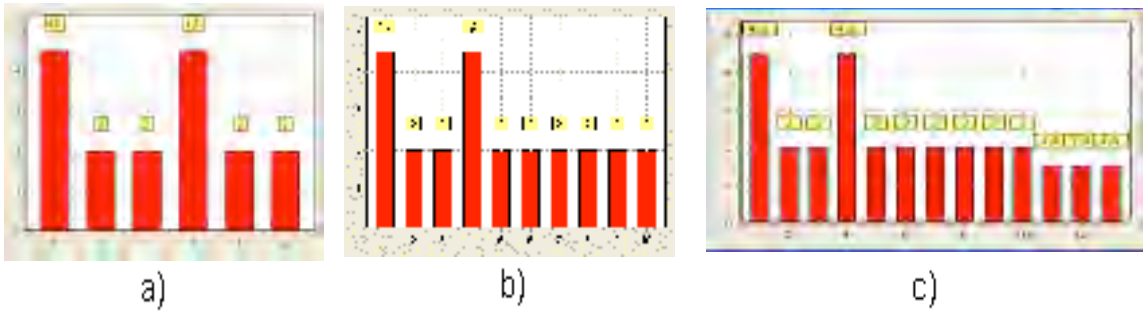

Fig. 2. Schemes of keyboard block uplift used for the numerical simulation: a) Sumatra segment; b) Sumatra and Nicobar segments; c) Sumatra, Nicobar and Andaman segments. The horizontal scale corresponds to the number of keyboard blocks (see Fig.1b), while the vertical scale corresponds to the magnitude of keyboard-block vertical shift (m); figures at the panels correspond to the maximum shift magnitude (in meters).

To accomplish the analysis, consider first the effect of length of underwater seismic source to the development and distribution of the initial tsunami wave field in the basin of the Bay of Bengal and in the central part of Indian Ocean. To analyze further the effect of each large segment of the seismic source that generated the tsunami and the formation of the wave field, it became necessary also to consider three independent contributing sources, namely the Sumatra segment, the Sumatra and Nicobar segments and the Sumatra, Nicobar and Andaman segments (see, Fig. 1b). The magnitudes of maximum keyboard-block displacements for the three seismic source scenarios that were considered are illustrated in Fig. 2. Fig. 3 illustrates the results of tsunami wave generation and propagation for each of these three scenarios. Also shown in this figure is the track and position of the satellite traversing the region (the white line) during this time period.

As shown in Fig. 3a, formed at the ocean surface tsunami source (for the first scenario), generates an almost circular wave pattern, which, due to the bathymetry of the basin, persists in form and propagates faster in a west and southwest direction. Toward the northwest of the Indian coast, the wave arrives with significant delay when compared with the actual recorded wave arrival at tide gauge stations. As seen from the wave field development based on the second scenario (Fig. 3b), the tsunami front becomes more elongated and the time of the first wave arrival on the east coast of India

is decreased - as compared with the case of wave generation only by Sumatra segment (First scenario). When the third segment is included (scenario 3) the wave field is characterized by still more elongated shape to north wave front (Fig. 3c) and the time of the first wave reaching the south-east coast of India is further decreased. It can be seen that along the source side facing the Bay of Bengal, there are three well defined wave fronts corresponding to the designated segments (Fig. 3c). These fronts then form a plane, united front with a subsequent bend in the region of the Nicobar Islands. The change in the character of the wave field for the three cases is well seen from the calculated satellite altimetry shown in Fig. 4.

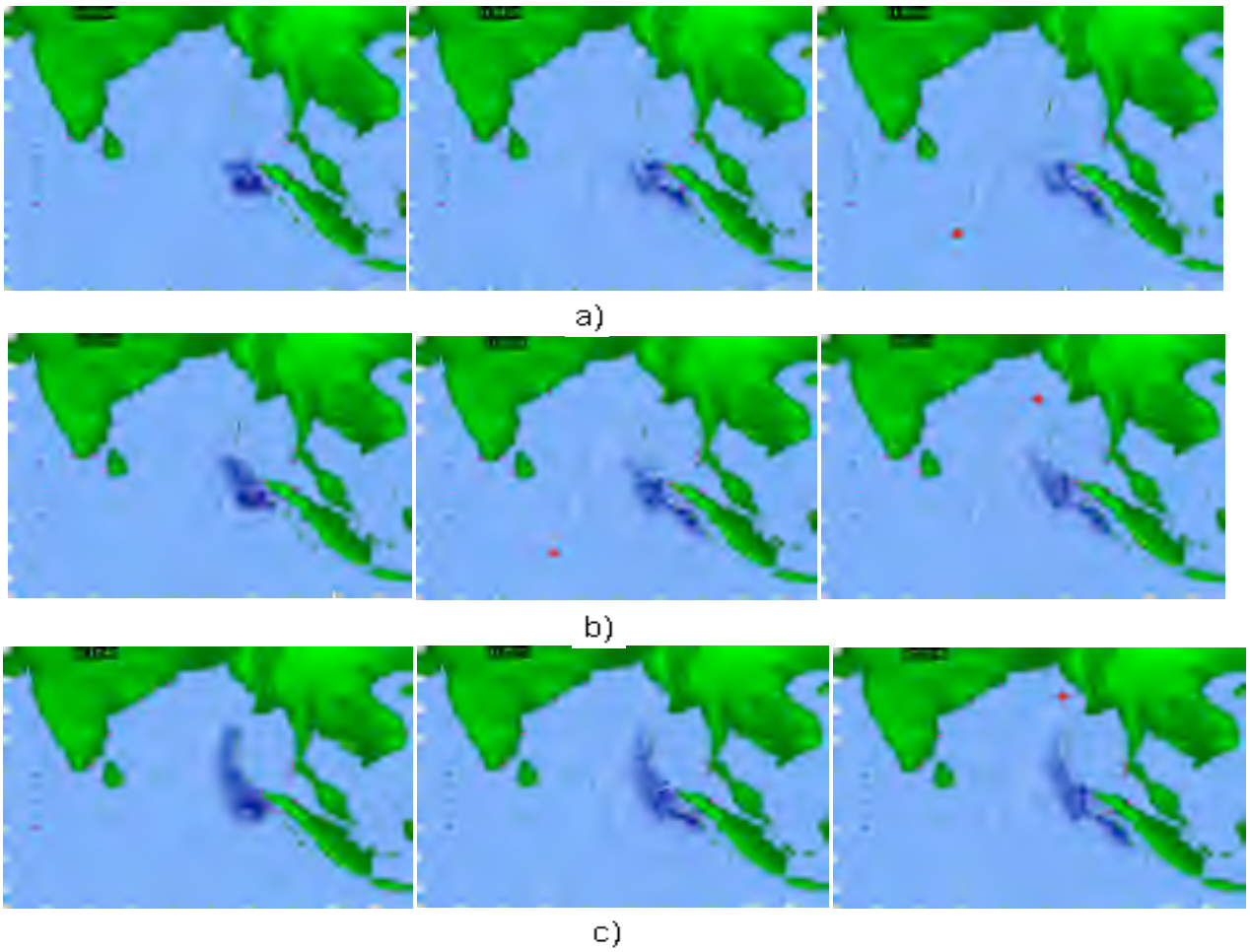

Fig. 3. The generation and propagation of tsunami wave on the Indian Ocean basin: scenario a) - 1; b) - 2; c) - 3. Red point at white line corresponds to the position of virtual satellite in time moment presented at panels

In the calculated picture of the wave field, corresponding to the satellite trajectory (Fig. 1a), some of the observed features appear to be only connected with wave generation by one segment (Fig. 4, upper panel). The characteristic feature is first a positive peak and essentially a larger, negative one.

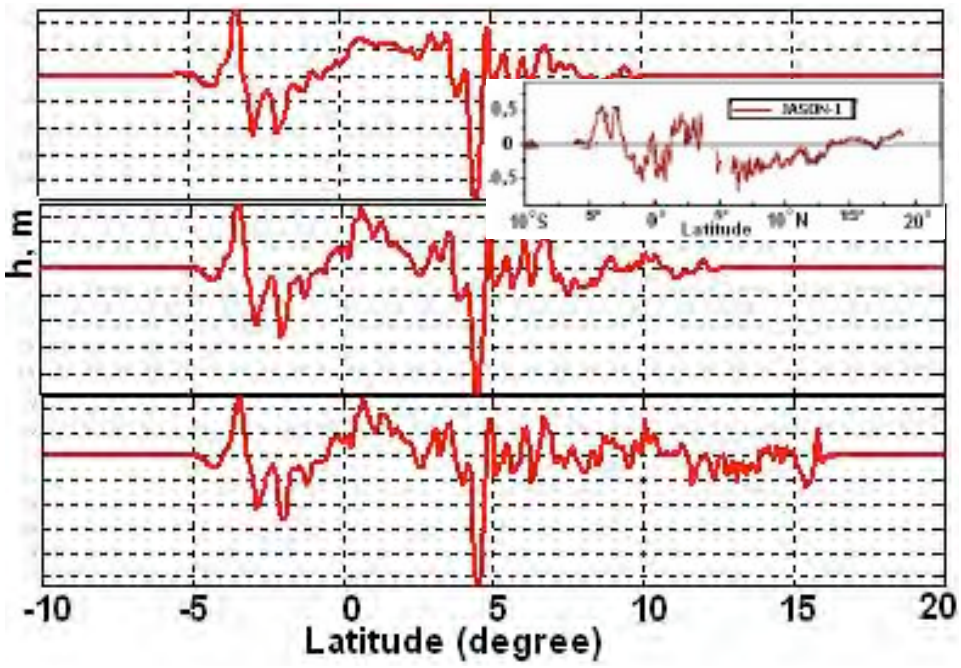

Fig. 4. The virtual satellite altimetry at numerical simulation with scenario 1, 2 and 3 (from up to down). Inset: the real altimetry from satellite "Jason-1".

When the second segment is included, it can be seen that there are changes in satellite altimetry, as a second positive wave is formed and the altimetric record is elongated (Fig.4, middle panel). The inclusion of third segment brings still more changes in altimetric record, although a number of characteristic features of wave fields persist. Therefore, the character of the leading wave, its height and its propagation in all three cases remain unchanged. However, it should be noted that there is a rise in the wave level behind the two negative peaks that are formed and that their amplitude is larger when compared with those exhibited with scenarios 1 and 2 (upper and middle panels). The characteristic negative peak, appearing already for scenario with only the Sumatra segment, is observed in all three calculations. However, in the third calculation its amplitude somewhat increases(lower panel). Also, it is well observed that with increasing of source length the satellite altimetric record is elongated and in the third case satellite fixes wave up to the moment of its passing the basin and its disappearance over the area. Thus, the wave field picture is in greater agreement with the results of satellite altimetric observations in both the region of the leading wave and, essentially, in the latitude region corresponding to the Nicobar Islands (Lay et al. 2005). Thus, the inclusion of the calculations of the second and third segments of the underwater seismic source, has no noticeable effect to leading wave, however, there appear significant changes in wave characteristics in the vicinity of the Nicobar and Andaman Islands as well as along the impacted coasts corresponding to these segments. As seen in Fig. 4 (lower panel), the calculated wave field picture corresponding to satellite trajectory is close to the observed altimetry of satellite "Jason-1" (see inset at Fig.4).

2.3 Numerical simulation of tsunami wave generation by seismic source comprising various numbers of keyboard blocks and subsequent wave propagation

To realize scenario 4, considered was a seismic source comprising 14 keyboard blocks and extending for 1400 km along the Sumatra-Nicobar-Andaman deep-sea trench. The keyboard blocks were 100 km long and 150 km wide. Their coordinates and sizes of the blocks were taken from the literature (Hirata et al. 2006), where such source was based on satellite data of sea surface height profiles and ocean floor rupture and deformation propagating to the north from Sumatra Island with very low velocity - less than 1 km/sec (in average). The scheme of movements of keyboard blocks for this scenario is presented in Table 1.

Table 1. Parameters of keyboard block movements for scenario 4

Block number	1	2	3	4	5	6	7	8	9	10	11	12	13	14
Shift value (m)	9	8	6	6	4	4	2	2	2	2	2	1,5	1,5	1,5
Shift time (Sec)	30	60	90	120	150	180	210	240	300	360	420	480	540	600

Shown in the second row of this Table are the maximum values of vertical shift for each of the keyboard blocks of the seismic source. Shown in the third line is the time of movement of each keyboard block. From the above Table, it can be seen that each keyboard block begins to move after the motion of the preceding block terminates. Also shown is that the first 8 blocks lift up to maximum height for about 30 seconds, but all subsequent blocks for 60 seconds. The total time of motion from south to north is 600 sec (10 min). Presented in Figure 5 below are six time steps during tsunami wave generation by the seismic source, comprising 14 keyboard blocks and moving sequentially from south to north. In two last figures the fixed positions of satellite "Jason-1" can be seen as it moves along its trajectory

The picture of maximum wave height distribution obtained from this simulation, demonstrates that the highest wave height was observed along Sumatra, the Indian coast, Sri-Lanka, the Maldives and along numerous other coastlines. – Qualitatively this is in good agreement with the actual observations and recordings of the event. Our preliminary analysis demonstrated that the vertical components of keyboard block shifts cannot exceed 9 meters since larger maximum uplift of keyboard blocks results in significantly larger vertical shifts of the free water surface in the Indian Ocean than those determined with the data from satellite "Jason-1". So, the given scenario at which rupture is directed successively from south to north and vertical shift reaches significant magnitudes (see above), obviously is not optimal.

On the basis of analysis of seismic and hydroacoustic data given in the literature (Ammon et al. 2005; Borges et al. 2005; Guilbert et al. 2005; Hirata et al. 2006; Ishii et al. 2005; Lay et al. 2005; Nagarajan et al. 2006; Park et al. 2005; Song et al. 2005; Titov et al. 2005; Park et al. 2005) different

scenarios were considered where the movement of the keyboard blocks in the seismic source was not only successive from south to north with various orientation of movements and different speeds, but was also alternating. Evaluation was performed of results of virtual satellite altimetry, obtained by us for each calculation.

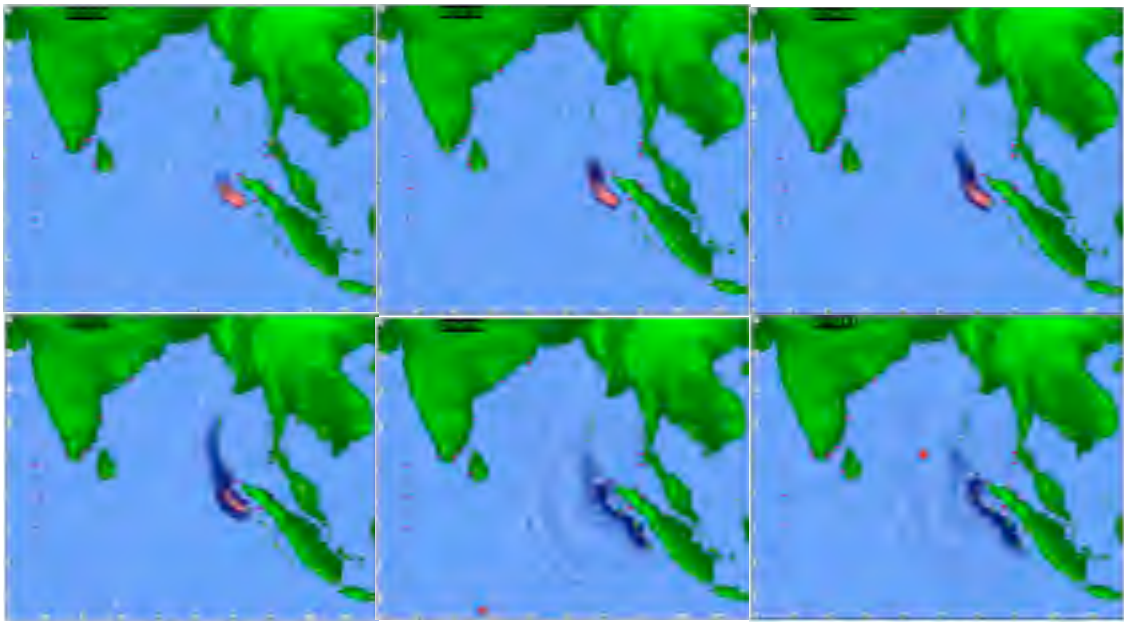

Fig. 5. Scenario 4. Tsunami wave generation from seismic source comprising 14 keyboard blocks.

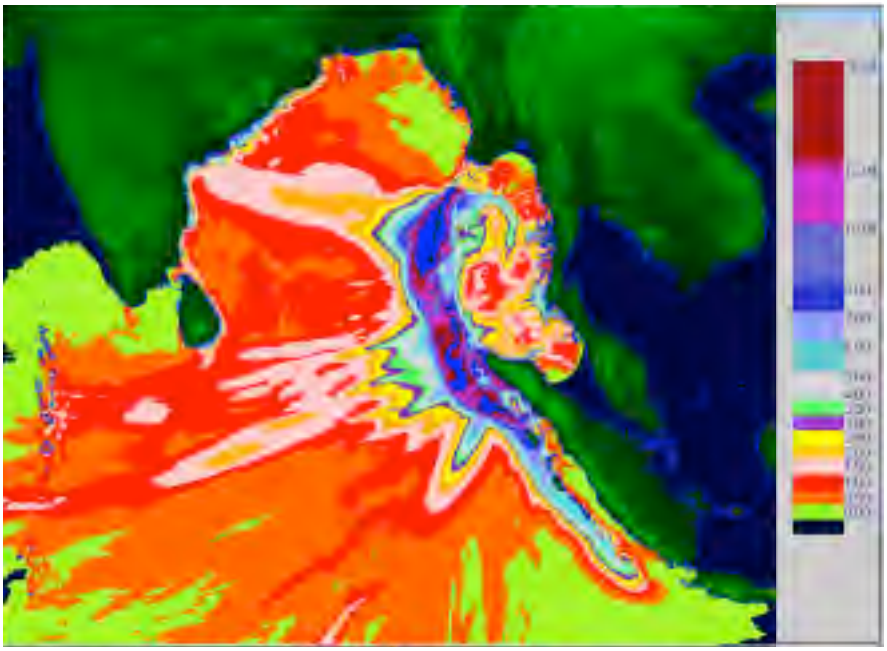

Fig. 6. Distribution of maximum tsunami wave height for scenario 4.

Shown in Figure 7 are three variants of the simulation: the upper panel corresponds to scenario 4, the middle one to scenario 5 and the lower one to scenario 6.

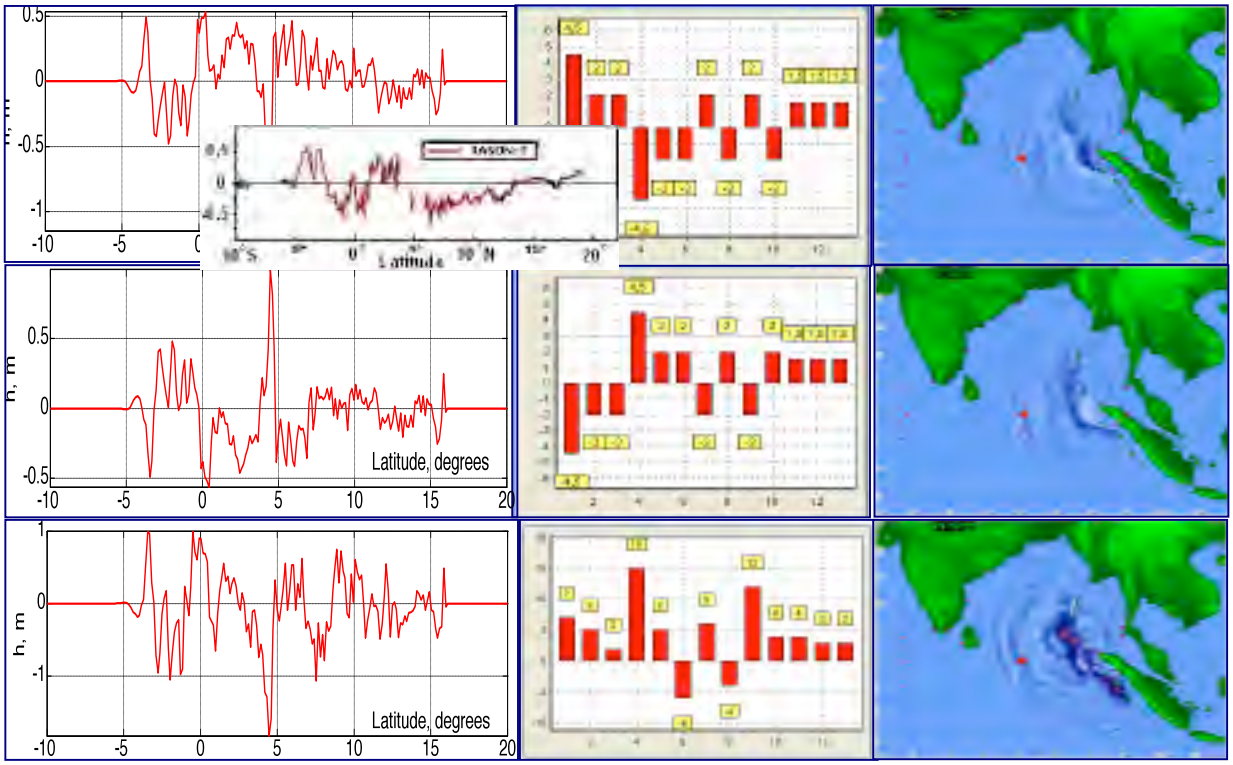

a) b) c)

Fig. 7. The results of numerical simulation with scenarios 5-7: a) virtual satellite altimetry with scenarios 5-7; b) sketch of location of keyboard blocks in seismic source; c) wave field distribution for each scenario; white direct line corresponds to the flight trajectory of satellite "Jason-1" and red dots on this line correspond to the position of satellite at given moment of time.

In Fig.7a presented are the results of model altimetric record at simulation of motion of virtual satellite along trajectory of real satellite "Jason-1". Shown in Figure 7b is a schematic view of the moment of maximum uplift of keyboard blocks. Figure 7c illustrates the calculated picture of wave field distribution and the position of the virtual satellite two hours and forty minutes after the main earthquake. According to scenarios 5-7, the seismic source - comprising three segments (see Fig. 1b) - is subdivided to the following blocks: the first segment is that of Sumatra (blocks 1-6), the second is that of the Nicobar Islands (blocks 7-10) and the third is that of the Andaman Islands (blocks 11-13). For scenario 5 the keyboard blocks with negative displacement (4, 5, 6, 8, 10) are oriented towards the Island of Sumatra and, in contrast to scenario 4, differ in vertical movement magnitude and in the sequence of keyboard block lifting. Scenario 6 is symmetrical to scenario 5, the motion of keyboard blocks being oriented downward towards the ocean (1-3, 7, 9), but the rest of the blocks move upward. To perform more adequate estimations, the magnitudes of maximum shifts of

keyboard blocks used for scenarios 5 and 6 were the same. For scenario 7, keyboard block displacement reached 15 m. Keyboard blocks with negative displacements (6 and 8) are oriented towards Sumatra (see, Table 2) but the motion of keyboard blocks begins from keyboard block 4 (see Table 2). As expected, the satellite altimetry of wave heights for both scenarios 5 and 6 is 'inverted'. However, for scenario 7, the wave train following the leading wave is characterized with large positive peaks. The significant negative tails, appearing behind the central positive part of the signal at the lifting of the first keyboard blocks up, are characteristic for scenarios 5 and 7.

Table 2**.** Parameters of keyboard block movements for scenario **7**

Block number	1	2	3	4	5	6	7	8	9	10	11	12	13
Shift value (m)	7	5	2	15	5	-6	6	-4	12	4	4	3	3
Start time (sec)	30	30	60	0	30	60	120	120	240	240	360	440	520
Stop time (sec)	120	60	180	30	240	300	300	360	360	360	480	480	600

For scenario 6, the altimetry obtained is qualitatively different of the real altimetry, which indicates the impossibility of such a scenario - where part of the seismic source facing the ocean is associated with negative movement. For scenarios 5 and 7, the change in the extent of displacements of the first keyboard blocks affects the behavior in the central part of the graphics - which in both cases can be explained by resonance effects at interaction of wave fronts coming from different segments. The picture of the wave field computed for scenario 5 is presented in Figure 8 where 9 time moments of tsunami generation and propagation from the seismic source are presented. It is well seen that the forming tsunami source (upper panels), is dipolar in character. Indeed, closer to the Island of Sumatra a depression is observed while on the open ocean side from the source an elevation of water surface is formed.

With increasing time, negative waves reached the coast of Sumatra, leading to a withdrawal of the water from the shore – which was indeed observed. However, the whole wave field character in the open ocean is consistent with the results of other studies. The computed frontal profile of sea surface height, during the passing of the tsunami wave, corresponded to the time and path trajectory of the satellite and the measurements in this scenario are essentially closer to the satellite data - as they relate to both the leading wave and the characteristic sharp depression of the ocean surface as determined by the satellite during its passage near the Nicobar Islands. This permits to suggest that such a scenario is closer to reality of the given structure of movements of the seismic source. However, it is necessary to note that satellite altimetry obtained in its tail part is somewhat different from the real record. In real altimetry the curve of the profile of sea surface height along the satellite's trajectory is located below the abscissa axis, which in fact indicates that for large part of its flight path, the satellite determined the depression of water level in the ocean.

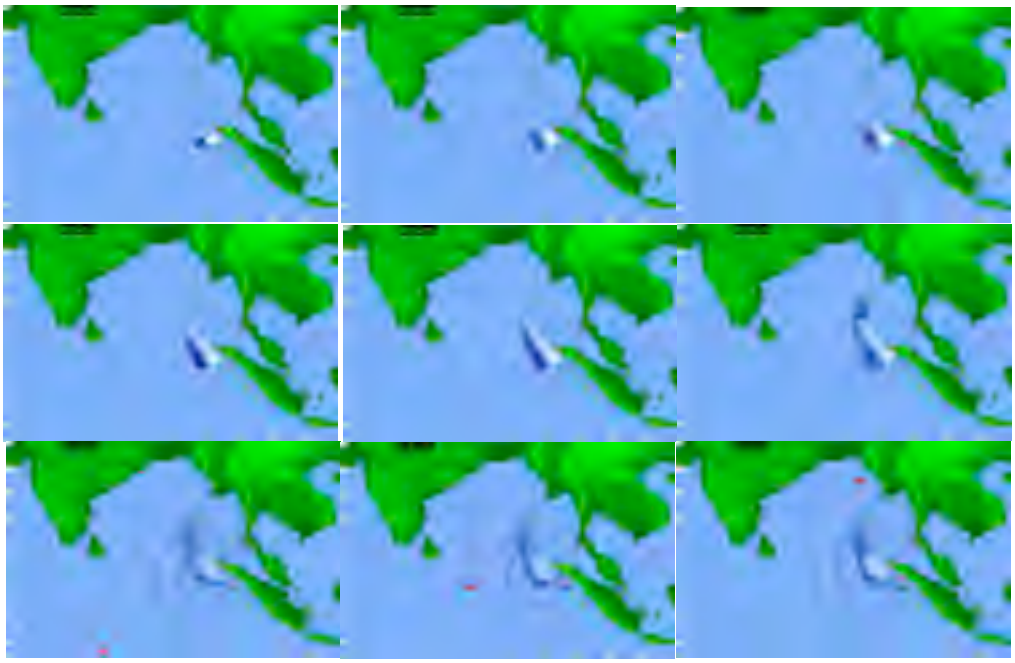

Fig. 8. Formation of tsunami source and propagation of tsunami wave in the Indian Ocean basin for scenario 5. At lower three panels; there are fixed time moments of the flight of the virtual satellite.

To approximate the character of the computed curve to the natural one, a numerical simulation was performed on scenario 8, which differs from those of scenarios 5 and 7 in the order of motion of some keyboard blocks. In scenarios 7 and 8, the setting of keyboard motions in the earthquake source approximated the results of other work (Ishii et al. 2005) (see, Table. 2 and 3) and is in the following order: $4 \rightarrow 2$, $1 \rightarrow 3 \rightarrow 5 \rightarrow 6$, $7 \rightarrow 8$, $9 \rightarrow 10 \rightarrow 11 \rightarrow 12 \rightarrow 13$.

Table 3. Parameters of keyboard block movements for scenario 8

Block number	1	2	3	4	5	6	7	8	9	10	11	12	13
Shift value (m)	4,5	2	2	-4,5	-2	-2	2	-2	2	-2	1,5	1,5	1,5
Start time (sec)	30	30	60	0	120	180	180	240	240	300	360	420	480
Stop time (sec)	120	60	180	30	240	300	300	360	360	360	480	480	600

The values of shifts are set somewhat less than for scenario 7 since the altimetric record of the satellite at simulation of scenario 7 results in essentially excessive magnitudes of sea surface height (see Fig. 7, lower panel). For scenario 8 the magnitudes of height in the altimetric record are closer to the real data (Figure 9).

Furthermore, the magnitude of the negative peak is decreased and the curve of sea surface height profile is located below the zero level - which corresponds better to the real altimetric record from satellite "Jason-1" as compared with the simulation on scenarios 5 and 7. Thus, a tendency of the source formation of the 26 December 2004 earthquake becomes better defined. A sequence of multi-block movements occurs along the source with the normal fault oriented towards Sumatra Island, while strong reverse fault is oriented on the ocean along the Sumatra segment of the source. The Nicobar segment of source normal fault is oriented towards Thailand and a reverse fault, somewhat weaker as compared with the Sumatra segment, is also oriented towards ocean. Thus, keyboard motion is not strictly successive from south to north.

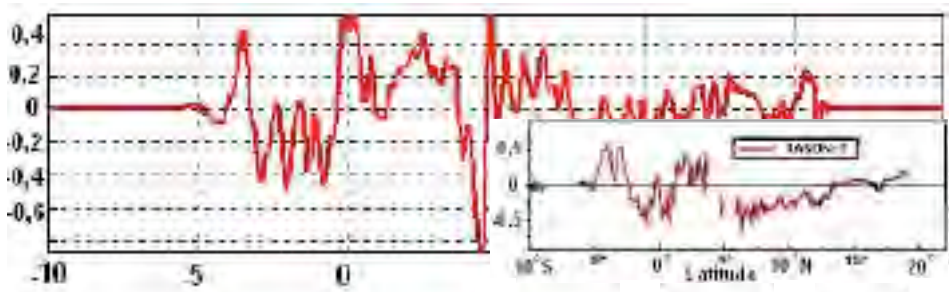

Fig. 9. The virtual satellite altimetry for scenario 8.

2.4 Spectral analysis of results of the numerical simulation of tsunami waves

The data about the change of surface water height obtained by satellite facilities were used to estimate spectral characteristics of tsunami waves in the open ocean, propagating towards India and Sri-Lanka. Using the above stated results, wavelet-analysis and comparison with spectrogram were performed with the available altimetry data of satellite "Yason-1" (Kulikov et al. 2005).

A spectral analysis of computed altimetry is shown in Figure 10 obtained for scenarios 4 and 7. Figure 11 illustrates the wavelet analysis for scenarios 1-3, which permits to estimate the influence of the length of seismic source to the wave characteristics of the tsunami in the open ocean with the use of computed satellite altimetry. From this, it becomes obvious that when the seismic source comprises only one segment (Sumatran one) (upper panel), then the low-frequency component is well localized in the interval ranging from 3S to 7N and is of significant intensity. This region corresponds to a wavelength of the order of 500 km. Around this region there are three, well defined zones of intensity (black and black-grey ovals). Upwards, black-grey regions occur with two characteristic peaks in regions of higher frequencies. When the second segment (Nicobar one) is included (middle panel), the low-frequency area is somewhat smoothed and becomes less intensive. However, there are significant distortions in the right part of spectrum, in the interval ranging from 5N to 10N, in the wavelength range of the order of 200 km. The low-frequency part of the spectrum is shifted to 15N. When the third segment (Andaman one) is included, the intensive low-frequency area is elongated to 7 N, while the less intensive area occurs at 15N. The next expressed frequency area is almost the same as in the case of the two segments and the frequency area at the level of 10^{-2} becomes more intensive.

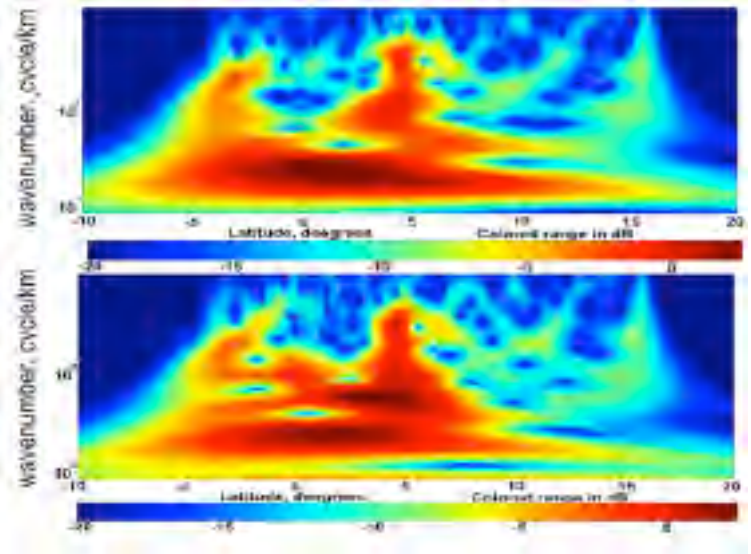

Fig. 10**.** Wavelet-analysis for altimetry, obtained at realization of scenarios 4 and 7.

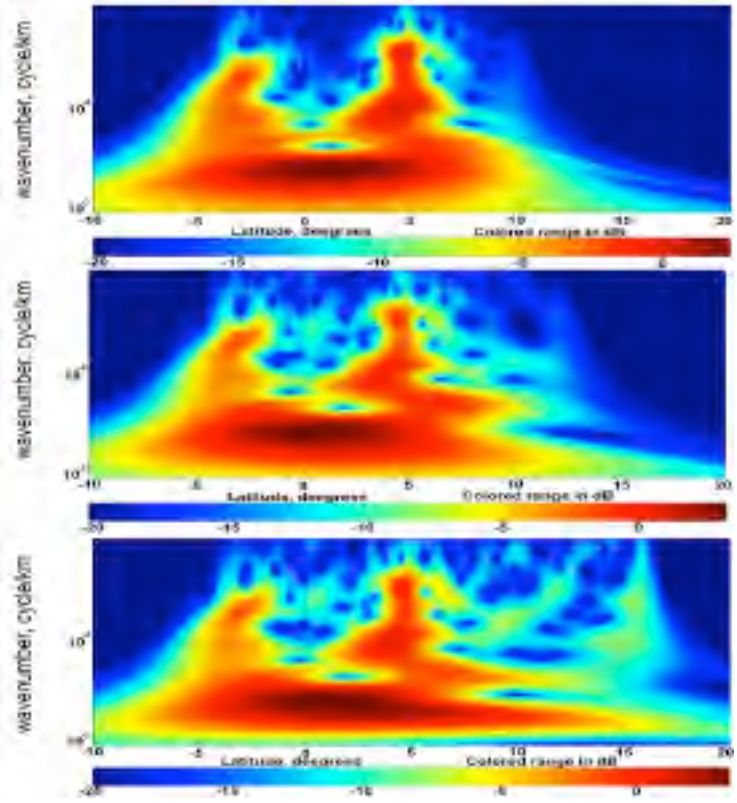

Fig.11.Wavelet-analysis for altimetry, obtained by analysis of influence of the length of the seismic source: upper panel – 1 segment; middle panel – 2 segments; lower panel – 3 segments (for more details, see the text).

It should be noted that for all three cases the left part of the spectrogram remained practically unchanged. It is well seen that low frequencies enter the region earlier than higher ones, which permits to conclude that it is consistent with findings (Kulikov et al. 2005) about the presence of high-frequency dispersion. In the spectrogram there are well-seen "large" and "small" hills coming on horizontals 0.02 and 0.05-0.06, respectively. It is also seen that a delay with the appearance of harmonic components increases with their wave numbers. The results of the present analysis demonstrate the importance of the effect of linear dispersion on the propagation and transformation of tsunami waves in the Indian Ocean and the necessity of taking into account this effect at numerically simulating tsunami wave propagation.

3. DISCUSSION AND CONCLUSION

The results of the numerical simulation demonstrate that by using the keyboard structure of an underwater earthquake source and by changing its dynamics, it is possible to obtain essentially a different wave field character for surface wave generation. With such a process of tsunami source formation, the magnitudes of maximum wave heights and their distribution on the shore can be determined. The estimations of wave height at 10 m isobate, even in a simplified model, give the opportunity to select the seismic source configuration. By using a simplified keyboard model and by taking into account the vertical components of keyboard block displacement of the seismic source, we were able to select the most possible kinematical process describing adequately the tsunami's wave field behavior in Indian Ocean basin for the given tsunami. It should be also noted that the motion of the keyboard blocks in the seismic source region is not successive from south to north and that the present analysis is consistent with results of numerous other studies. Furthermore, the use of different scenarios of kinematic motions of keyboard blocks in the seismic source region used in the present study, permitted the determination of the optimal source parameters that were responsible for tsunami generation and to conclude what the best-fit source was. It also helped illustrate that the most adequate formation of the earthquake source responsible for the tsunami was when the normal fault is oriented towards the Island of Sumatra and the strong reverse fault occurred towards the ocean side of the Sumatra segment of the source, while in the Nicobar segment of the source, the normal fault is oriented towards Thailand, but with somewhat weaker reverse fault than that along the Sumatra segment oriented towards the open ocean. It is necessary also to note that using of wavelet analysis of altimetric records of virtual satellite flights for each scenario permitted the confirmation of our suggestion on the probability of realization of such scenario.

Acknowledgments

The present study was supported by the Russian Foundation for Basic Research, project no. 12-05-00808.

The authors appreciate Dr. George Pararas-Carayannis' critical reading and careful editing.

REFERENCES

Ammon C.J., C.Ji, H.-K. Thio, D.Robinson, S.Ni, V.Hjorleifsdottir et al., 2005. Rupture Process of the Great Sumatra-Andaman Earthquake // *Science* 308, 1133-1139.

Borges J.F., Caldeira B., and M.Bezzeghoud, 2005. Source rupture process of the great Sumatra, Indonesia earthquake (M_w=8.9) of 26 December 2004 (Preliminary Results), *unpublished*) 1-6.

De Groot-Hedlin C.D., 2005. Estimation of the rupture length and velocity of the great Sumatra earthquake of Dec 26, 2004 using hydroacoustic signals, *Geophysical Research Letters* 32, L11303 (1-4).

Guilbert J., Verzog J., Schissele E., Roueff A., and Y.Cansi, 2005. Use of hydroacoustic and seismic arrays to observe rupture propagation and source extent of the M = 9.0 Sumatra earthquake, *Geophysical Research Letters* 32, L15310 (1-5).

Hirata K., Satake K., Tanioka Y., Kuragano T., Hasegawa Y., Hayashi Y., and N. Hamada, 2006. The 2004 Indian Ocean tsunami: tsunami source model from satellite altimetry, *Earth Planets Space* 58(3), 195-201.

Ishii M., Shearer P.M., Houston H., and J.E.Vidale, 2005. Extent, duration and speed of the 2004 Sumatra-Andaman earthquake imaged by the Hi-Net Array, *Nature* 435, 933-936.

Lay T., Kanamori H., Ammon C.J., Nettless M., Ward S.N., Aster R.C., et al., 2005. The Great Sumatra-Andaman Earthquake of 26 December 2004, *Science* 308, 1127-1133.

Lobkovsky L.I., 1988 *Geodynamics of spreading and subduction zones, and two-level plate tectonics* (Moscow, Nauka Press).

Lobkovsky L.I., Nikishin A.M., and V.T.Khain, 2004. *Current problems of geotectonics and geodynamics* (Moscow, Scientific World).

Lobkovsky, L. I., R. Kh. Mazova, I. A. Garagash, L. Yu. Kataeva, and I. Nardin 2006a To analysis of source mechanism of the 26 December 2004 Indian Ocean tsunami, *Russ. J. Earth Sci.*, V.8, ES5001, doi:10.2205/2006ES000208.2006 http://dx.doi.org/10.2205/2006ES000208,

Lobkovsky L.I., Mazova R.Kh., Kataeva L.Yu., and B.V.Baranov, 2006b. Generation and propagation of catastrophic tsunami in the Sea of Okhotsk basin. Possible scenarios, *Doklady RAS* 410, 528-531.

Lobkovsky L.I., and R.Kh.Mazova, 2007. Source mechanism of the tsunami of 2004 in the Indian Ocean: analysis and numerical simulation, Izvestiya. Physics of the Solid Earth 43, 573- 582.

Nagarajan B., Suresh I., Sundar D., Sharma R., Lal A.K., Neetu S., et al., 2006. The Great Tsunami of 26 December 2004: A description based on tide-gauge data from the Indian subcontinent and surrounding areas, *Earth Planets Space*, 58, 211–215.

Park J., Song T.-R.A., Tromp J., Okal E., Stein S., Roult G., et al., 2005. Earth's free oscillations excited by the 26 December 2004 Sumatra-Andaman earthquake, *Science* 308, 1139-1146.

Song Y.T., Li C., Fu L.-L., Zlotnicki V., Shum C.K., Yu Y, and V.Hjorleifsdottir, 2005. The 26 December 2004 tsunami source estimated from satellite radar altimetry and seismic waves, *Geophysical Research Letters* 32, L20601-5.

Tanioka Y., Yudhicara Y., Kususose T., Kathiroli S., Nishimura Y., Iwasaki S.-I., and K.Satake, 2006. Rupture process of the 2004 great Sumatra-Andaman earthquake estimated from tsunami waveforms, *Earth Planets Space*, 58, P.1–7.

Titov V., Rabinovich A.B., Mofield H.O., Thomson R.E., and F.I.Gonzalez, 2005. The global reach of the 26 December 2004 Sumatra tsunami, *Science* 309, 2045-2048.

Wilson M., 2005. Modeling the Sumatra-Andaman Earthquake reveals a complex, nonuniform rupture, *Phys.Today*, June, 19-21.

Kulikov E.A., Medvedev P.P., and S.S.Lappo, 2005. Registration from cosmos of tsunami 26 December 2004 in Indian Ocean, *Doklady RAS* 401, 537-542.